

## Spin Echo Measurements of Nuclear Spin Coupling in Molecules\*

E. L. HAHN†‡ AND D. E. MAXWELL  
*Stanford University, Stanford, California*

(Received August 4, 1952)

A new type of nuclear spin-spin coupling in molecules in liquids is investigated by means of the spin echo technique. A coupling interaction of the rotationally invariant form  $\hbar J \mathbf{I}_1 \cdot \mathbf{I}_2$  in the nuclear induction Hamiltonian predicts the detailed shape of the spin echo envelope. Echo modulation frequencies corresponding to the coupling  $J$  and the chemical shift between nonequivalent protons are measured in a variety of compounds. A generalized method for calculating the spin echo is presented for large chemical shift and weak coupling among an arbitrary number of spins. The damping of the echo modulation, due to spin relaxation and molecular effects which interrupt the  $J$  coupling, is accounted for by a phenomenological treatment of the quantum-mechanical expectation value of nuclear magnetization.

### I. INTRODUCTION

ASIDE from the measurement of spins and gyromagnetic ratios by the method of nuclear resonance or nuclear induction,<sup>1,2</sup> there are many problems in molecular structure and the solid state which have been studied by this technique. This paper deals primarily with one of a group of higher order effects determined by the chemical environment of the nucleus. The nuclear configurations in crystals and the electronic configurations about nuclei in atoms, molecules, and in metals cause definite shifts in the nuclear resonance frequency. The resonance frequency of the nuclear moment is shifted from that value which it would have if the nucleus were isolated from neighboring nuclei, and stripped of all extra-nuclear electrons. In some instances a single resonance line may be split into two or more lines by local magnetic fields in the lattice, or an electric field gradient may interact with any nuclear electric quadrupole moment and cause line splitting. In the case of single resonance shifts, actual experiment reveals the differences in absolute shifts between resonance frequencies of like nuclear species as they occur in different chemical environments. An outline of the known effects which produce resonance shifts is given below.

#### A. The Chemical Shift

A shift in the nuclear resonance, known as the chemical shift,<sup>3,4</sup> is due to the effects of diamagnetism and induced paramagnetism in a molecule. Because these two effects are linearly proportional to the applied magnetic field, it is impossible to distinguish them from one another. A local magnetic field at the position of the nucleus is caused by the Larmor precession of extra-nuclear electrons in an externally applied magnetic field. In first order, the effect due to a spherically

symmetric electron distribution is given by the Lamb diamagnetic correction.<sup>5</sup> In second order, where electrons undergo attraction by two or more nuclei in molecules, it has been shown by Ramsey<sup>6</sup> that the induced paramagnetism (which in many cases is comparable to, or larger than, the diamagnetic correction) arises from a perturbation in which the ground state mixes with a paramagnetic excited state of the molecule. This causes the observed large chemical shift when the energy level of the paramagnetic state lies very close to that of the ground state.

#### B. Direct Nuclear Magnetic Dipole-Dipole Coupling in Crystals

Pake first showed<sup>7</sup> that the resonance of two proton nuclear moments, which are close neighbors, reveals a splitting into two lines. The magnetic dipole fields, due to parallel and antiparallel orientations of the protons, respectively add and subtract local fields at the positions of these protons throughout the lattice. These values superimpose upon the constant value of the externally applied field and cause the splitting. More complicated spin systems in crystals have been studied which show resonance line shapes determined by the direct dipole-dipole interaction.<sup>8</sup> No case has been confirmed in which the direct interaction prevails in liquids. This is to be expected since this direct coupling averages out due to rapid and random rotations of a molecule in a liquid.<sup>1,9</sup>

#### C. Shift Due to Conduction Electrons in Metals

Knight<sup>10</sup> has found that the paramagnetism due to conduction electrons in metals causes a net local mag-

<sup>5</sup> W. E. Lamb, Phys. Rev. **60**, 817 (1941).

<sup>6</sup> N. F. Ramsey, Phys. Rev. **78**, 699 (1950).

<sup>7</sup> G. E. Pake, J. Chem. Phys. **16**, 327 (1948).

<sup>8</sup> E. R. Andrew and R. Bersohn, J. Chem. Phys. **18**, 159 (1950).

<sup>9</sup> The interaction between two parallel dipoles is proportional to  $1-3\cos^2\theta$ , where  $\theta$  is the angle between the internuclear axis and the direction of the dipoles. This quantity averages to zero over a sphere but its square does not. During discussions at the American Physical Society meeting in Washington, D. C., April, 1951, Purcell pointed out that for this reason the direct interaction, in second order, can exist in liquids with a magnitude inversely proportional to the applied magnetic field. As yet this small effect has not been observed.

<sup>10</sup> W. D. Knight, Phys. Rev. **76**, 1259 (1949).

\* Supported in part by the ONR.

† National Research Council Post-doctoral Fellow during a portion of this research.

‡ Present address: Watson Computing Laboratory, Columbia University, New York 27, New York.

<sup>1</sup> Bloembergen, Purcell, and Pound, Phys. Rev. **73**, 679 (1948).

<sup>2</sup> F. Bloch, Phys. Rev. **70**, 460 (1946).

<sup>3</sup> W. G. Proctor and F. C. Yu, Phys. Rev. **77**, 717 (1950).

<sup>4</sup> W. C. Dickenson, Phys. Rev. **77**, 736 (1950).

netic field at the position of the nucleus. The magnitude of this shift is proportional to the value of the applied magnetic field.

#### D. Quadrupole Splitting in Crystals

Pound has demonstrated<sup>11</sup> for nuclei with spin  $I > \frac{1}{2}$  that the gradient of the electric field at the nucleus in crystals splits the magnetic resonance into  $2I$  lines. In liquids electric field gradients have zero average value, and only a broadening of a single resonance line can result because of the quadrupole interaction.

#### E. Indirect Nuclear Spin-Spin Coupling

A new type of splitting is observed in liquids which is independent of the applied magnetic field and the temperature. The bonding electrons between nuclear magnetic dipoles in a molecule serve as a medium which communicates a nuclear spin-spin magnetic interaction. The first case of such a field independent splitting was observed by the slow passage method in  $\text{Sb}^{121}$  contained in the  $\text{SbF}_6^-$  ion.<sup>12</sup> The effect was first attributed<sup>12,13</sup> to various local fields due to the possible  $\text{F}^{19}$  nuclear orientations (direct dipole coupling discussed in B above) which could split the  $\text{Sb}^{121}$  resonance into a number of lines. This requires the assumption that a hindrance of the random rotation of the  $\text{SbF}_6^-$  ion takes place in the liquid state so that the dipole fields due to the six  $\text{F}^{19}$  nuclei do not average out completely at the position of the  $\text{Sb}^{121}$  nucleus. The effect of such a splitting with use of spin echoes was later found in ethanol<sup>14</sup> and similar organic compounds. With the subsequent appearance of many cases of such splittings in liquids by the groups at Illinois<sup>15-17</sup> and at Stanford,<sup>18,19</sup> it became apparent that, although the direct nuclear dipole coupling mechanism might explain some general features of this splitting, the following difficulties arise: (a) it is difficult to account for rotational hindrance in a wide variety of molecules in liquids; and (b) the absence of splitting among chemically equivalent nuclear moments is not explained by this interaction.

Previously the authors have reported a measurement<sup>18</sup> of the spin echo envelope due to two coupled protons in dichloroacetaldehyde. An interaction of the form  $J'\mathbf{u}_1 \cdot \mathbf{u}_2$  was used in the Hamiltonian to predict the shape of the echo envelope in this molecule, and precise agreement was obtained with experiment. We may express  $J'\mathbf{u}_1 \cdot \mathbf{u}_2 = \hbar J \mathbf{I}_1 \cdot \mathbf{I}_2$ , where  $\mathbf{I} \equiv \mathbf{I}(I_x, I_y, I_z)$  is the

spin operator and  $J$  is expressed in angular frequency. This form of the interaction is invariant to rotation, which predicts the fact that the coupling can be observed in molecules in liquids. A generalized form of this operator correctly accounts for the number, relative amplitudes, and relative splittings of absorption lines observed by the slow passage method<sup>15</sup> when coupling takes place between nonequivalent groups of nuclear dipoles in the same molecule. No splitting or echo modulation is predicted by such a coupling between equivalent spins, although the coupling still exists.

Several specific spin-electron-spin coupling mechanisms are possible in molecules. A majority of them give rise to the  $\mathbf{u}_1 \cdot \mathbf{u}_2$  form of interaction and may all play a role in accounting for observed values of  $J$  of the order of 1 cps or less. In order to account for larger values of  $J$  observed in many cases (of the order of kilocycles), Ramsey and Purcell<sup>20</sup> have shown that the  $\mathbf{u}_1 \cdot \mathbf{u}_2$  interaction is due mainly to one mechanism which can make  $J$  so large that probably all other mechanisms are of negligible influence in most of the observed cases. In the example of two indirectly coupled moments in the HD molecule, Ramsey and Purcell have shown that the bonding electrons, with spins normally antiparallel, are parallel in the triplet state for a small percentage of the time because of the perturbing influence of parallel orientations of the H and D nuclei. The hyperfine interaction of the electrons with the H and D nuclei then cause net local magnetic fields to appear at the positions of these nuclei. The energy expression  $J'\mathbf{u}_1 \cdot \mathbf{u}_2$  thus accounts for the fact that nucleus 1 sees a local field proportional to  $J'\mu_2$  and conversely for nucleus 2, where  $J'$  accounts for the mechanism by which the bonding electrons communicate such a local field. In frequency units ( $J/2\pi$ ), each nucleus will see the same splitting, which Ramsey and Purcell have calculated to be approximately 70 cps for the HD molecule.

In this paper a transient analysis of the indirect spin-spin coupling effect (hereafter denoted by  $J$  coupling or splitting) is made of spin echo measurements.<sup>14</sup> The equivalent information in many respects is available from the analysis of steady-state resonance experiments, and yet the two methods serve to supplement each other. Many points which are discussed in this paper have been arrived at independently by the Gutowsky-Slichter group at Illinois.<sup>17</sup> In the course of our research we have learned, through exchange of information with the Illinois group, of the important results which they established from slow passage experiments.

The echo method possesses certain inherent advantages. For long relaxation times this method is able to resolve frequencies of the order of 1 cps, although an external field inhomogeneity over the spin sample produces a spread in Larmor frequencies much greater than this. Resolution is primarily limited because

<sup>11</sup> R. V. Pound, Phys. Rev. **79**, 685 (1950).

<sup>12</sup> W. G. Proctor and F. C. Yu, Phys. Rev. **81**, 20 (1951).

<sup>13</sup> E. R. Andrew, Phys. Rev. **82**, 443 (1951).

<sup>14</sup> E. L. Hahn, Phys. Rev. **80**, 580 (1950).

<sup>15</sup> H. S. Gutowsky and D. W. McCall, Phys. Rev. **82**, 748 (1951).

<sup>16</sup> Gutowsky, McCall, and Slichter, Phys. Rev. **84**, 589 (1951); McNeil, Slichter, and Gutowsky, Phys. Rev. **84**, 1245 (1951).

<sup>17</sup> Gutowsky, McCall, and Slichter, J. Chem. Phys. (to be published). We are grateful to them for an advance copy of this paper.

<sup>18</sup> E. L. Hahn and D. E. Maxwell, Phys. Rev. **84**, 1246 (1951).

<sup>19</sup> M. E. Packard and J. T. Arnold, Phys. Rev. **83**, 210 (1951); Arnold, Dharmatti, and Packard, J. Chem. Phys. **19**, 507 (1951).

<sup>20</sup> N. F. Ramsey and E. M. Purcell, Phys. Rev. **85**, 143 (1952).

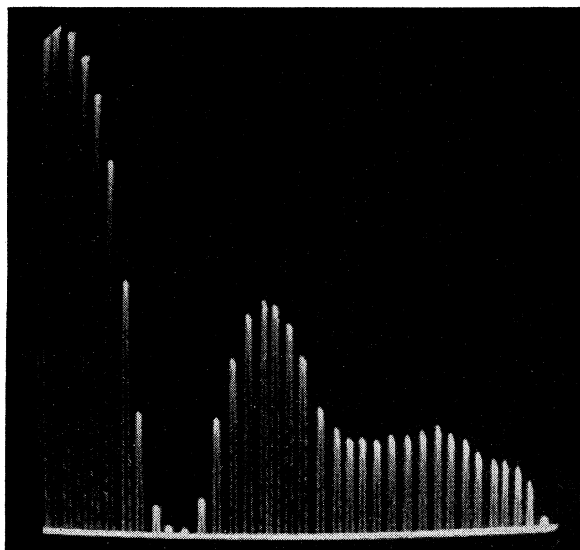


FIG. 1. Multiple photographic exposures of proton echo oscilloscope signals obtained in 2-bromo-5-chlorothiophene. The first rf pulse initiates the sweep. An exposure is made of the echo for each position of the second pulse (the pulses are not visible). As  $\tau$  is increased, the maximum of the spin echo at the time  $2\tau$  traces out the modulation of the echo envelope. The time duration of the total sweep is 0.66 sec, and the Larmor frequency is 31 Mc.

thermal self-diffusion of molecules in liquids destroys the coherence of precession frequency as the nucleus migrates from one field value to another. This effect, however, is not as serious as that due to field inhomogeneity in slow passage experiments. In experiments where the effect of small splittings must be resolved, and where theory must be checked in detail, it is advantageous to study echo signals because they occur in the absence of a driving rf field. Accurate information can be obtained from the detailed shape of the echo envelope without having to consider the effect of a driving rf field on the measured decay of the echo signal.

## II. THEORY AND EXPERIMENT OF THE TWO-PROTON COUPLING CASE

The majority of nuclear resonance effects observed in an ensemble of nuclear moments in a liquid are well described by the classical Bloch equations.<sup>2</sup> The longitudinal relaxation time  $T_1$  and the transverse relaxation time  $T_2$  can be measured as definite quantities providing that the nuclei are perturbed only by local fields which are completely random and isotropic. With the presence of  $J$  type coupling between nuclei within molecules in liquids, it is no longer possible to develop a general set of classical nuclear induction equations from the quantum-mechanical expectation values of the components of nuclear magnetization which are measured. Although the purely quantum-mechanical treatment which is to be presented shall at first not include the damping effect due to  $T_1$  and  $T_2$ , a phenomenological treatment, which uses the quantum-mechanical result,

will show that the over-all effect of these relaxation times is the same as in the Bloch equations; the coherence of the additional Larmor precession frequencies caused by the  $J$  splitting is also given by  $T_2$  and is destroyed exponentially.

According to the echo method,<sup>14</sup> two short, intense pulses of radiofrequency power are applied to the spin ensemble at resonance and are separated by the time interval  $\tau$ . The echo appears with a maximum amplitude at time  $2\tau$  after the application of the first pulse. At the onset of the first radiofrequency pulse the spin ensemble is at thermal equilibrium. For each setting of  $\tau$  the maximum of the echo signal is measured and plotted as a function of increasing  $\tau$ . The echo envelope thus obtained will normally decay monotonically with time in the absence of  $J$  splitting, and can yield an accurate measure of  $T_2$  in those cases where molecular self-diffusion is not important. Consider now the simplest case of  $J$  splitting in which two resonant protons are close neighbors in a molecule, and in addition are chemically nonequivalent. This is denoted by assigning to proton 1 an absolute chemical shift of  $h_1$  gauss, and to proton 2 the value  $h_2$ . The  $J$  splitting is not observed unless coupled nuclei are nonequivalent in the sense that (1) they have different chemical shifts, as in this particular case for identical nuclei, or (2) that they are not identical. The reason for this can be understood in the case of two-proton coupling where the  $J$  splitting appears in transitions between pure triplet states and states which are linear combinations of singlet and triplet terms. Normally transitions to the singlet state are forbidden unless the identity between the two protons is removed by a difference in chemical shift. With a chemical shift, as seen in Fig. 1, two frequencies then appear to modulate the decay of the spin echo envelope, which depend upon both  $J$  and  $\delta = \gamma(h_1 - h_2)$ , where  $\delta$  is the angular frequency which corresponds to the chemical shift and  $\gamma$  is the nuclear gyromagnetic ratio. The shape of this echo envelope can be described (as well as properties of  $J$  splitting observed in slow passage experiments) if the Hamiltonian,<sup>18</sup>

$$\mathcal{H} = -\gamma\hbar[\mathbf{I}_1 \cdot (\mathbf{H}_0 + \mathbf{h}_1) + \mathbf{I}_2 \cdot (\mathbf{H}_0 + \mathbf{h}_2)] - \hbar J \mathbf{I}_1 \cdot \mathbf{I}_2, \quad (1)$$

is chosen to describe the two-proton coupled system in a constant magnetic field  $H_0$ . Both nuclei are subjected to the nuclear resonance imposed by the application of two radiofrequency pulses, where the rf frequency  $\omega = \gamma H_0$ . Each pulse at  $H_1$  gauss maximum amplitude lasts for  $t_w$  seconds, where  $t_w \ll \tau$ , and  $1/t_w, \gamma H_1 (= \omega_1) \gg \gamma \Delta H, \delta, J$ ;  $\Delta H$  is the magnitude of the external field inhomogeneity over the sample. If only one of two coupled nuclei is subjected to resonance (e.g., between  $F^{19}$  and H) no echo envelope modulation will appear for either of such coupled nuclei, although the steady state resonance will still reveal the  $J$  splitting.

The zero order two-proton spin wave function, which applies both in the presence and absence of pulses, is

given by

$$\psi = \sum_{S=0}^1 \sum_{m=-S}^{-S} a_{S,m}(t) \phi_{S,m} \exp(-iE_{S,m}t/\hbar), \quad (2)$$

where the total spin  $S=1$  for the triplet state and  $S=0$  for the singlet state.  $\phi_{S,m}$  specifies the spin state function characterized by the magnetic quantum number  $m$ , and  $E_{S,m}$  is the corresponding eigenvalue. The three triplet state probability amplitudes  $a_{1,m}$  ( $m=1, 0, -1$ ) are time dependent during the application of  $H_1$  and the singlet state amplitude  $a_{0,0}$  remains constant. The Hamiltonian,

$$\mathcal{H} = -\gamma\hbar(\mathbf{I}_1 + \mathbf{I}_2) \cdot (\mathbf{H}_0 + \mathbf{H}_1), \quad (3)$$

describes the system during a pulse, and terms due to  $\delta$  and  $J$  are omitted for  $1/t_w \gg \delta$  and  $J$ . Upon substituting (2) and (3) into the time-dependent Schrödinger equation,

$$i\hbar\dot{\psi} = \mathcal{H}\psi, \quad (4)$$

and solving for  $a_{1,m}(t)$ , we obtain

$$a_{1,0}(t) = a_{1,0}(t_i) \cos(\omega_1 t) + (i/\sqrt{2}) \times [a_{1,1}(t_i) + a_{1,-1}(t_i)] \sin(\omega_1 t), \quad (5a)$$

$$a_{1,\pm 1}(t) = a_{1,\pm 1}(t_i) \cos^2(\omega_1 t/2) - a_{1,\mp 1}(t_i) \sin^2(\omega_1 t/2) + \frac{i}{\sqrt{2}} a_{1,0}(t_i) \sin(\omega_1 t). \quad (5b)$$

The pulse is turned on at  $t=t_i$  and turned off at  $t=t_i+t_w=t_i'$ . These coefficients can also be obtained from a general method given by Bloch and Rabi,<sup>21</sup> which will be applied later in cases involving more than two spins. In the absence of  $H_1$ , during the relatively long time of free Larmor precession, it is necessary to correct the wave function given by (2) in order to include the perturbation effects of  $\delta$  and  $J$  on the Larmor precession. The Hamiltonian given by (1) shall apply. The coefficients  $a_{S,m}$  become constants determined by initial conditions due to pulses. By the Ritz variational method<sup>22</sup> the following normalized and corrected wave function is obtained:

$$\psi = a_{1,1}(t_i') [\exp(-iE_{1,1}t/\hbar)] \alpha_1 \alpha_2 + a_{1,-1}(t_i') [\exp(-iE_{1,-1}t/\hbar)] \beta_1 \beta_2 \quad (6a)$$

$$+ \frac{1}{\sqrt{2}} \left( \frac{a_{0,0}(t_i') - a_{1,0}(t_i') Q'}{Q - Q'} \right) [\alpha_1 \beta_2 (1+Q) + \alpha_2 \beta_1 (1-Q)] \exp(-iE_0 t/\hbar) \quad (6b)$$

$$- \frac{1}{\sqrt{2}} \left( \frac{a_{0,0}(t_i') - a_{1,0}(t_i') Q}{Q - Q'} \right) [\alpha_1 \beta_2 (1+Q') + \alpha_2 \beta_1 (1-Q')] \exp(-iE_0' t/\hbar), \quad (6c)$$

<sup>21</sup> F. Bloch and I. I. Rabi, *Revs. Modern Phys.* **17**, 237 (1945).

<sup>22</sup> L. Pauling and E. B. Wilson, *Introduction to Quantum Mechanics* (McGraw-Hill Book Company, Inc., New York, 1935), p. 189.

where

$$Q = [J - (J^2 + \delta^2)^{1/2}] / \delta, \quad Q' = [J + (J^2 + \delta^2)^{1/2}] / \delta,$$

$$E_{1,1} = -\gamma\hbar(H_0 + \frac{1}{2}h_1 + \frac{1}{2}h_2) - \frac{1}{4}\hbar J,$$

$$E_{1,-1} = \gamma\hbar(H_0 + \frac{1}{2}h_1 + \frac{1}{2}h_2) - \frac{1}{4}\hbar J,$$

$$E_0 = \hbar[\frac{1}{4}J - \frac{1}{2}(J^2 + \delta^2)^{1/2}],$$

$$E_0' = \hbar[\frac{1}{4}J + \frac{1}{2}(J^2 + \delta^2)^{1/2}],$$

and  $\phi_{S,m}$  is a product function of component spin states of the system, with each state given by  $\alpha$  for  $I=\frac{1}{2}$  and  $\beta$  for  $I=-\frac{1}{2}$ . The constants  $a_{1,m}(t_i)$  of Eqs. (5) and  $a_{0,0}(t_i)$  are amplitudes of the above four stationary states at  $t=t_i$ . The coefficients of  $\alpha_1\alpha_2$ ,  $\beta_1\beta_2$ , and  $(\alpha_1\beta_2 + \alpha_2\beta_1)\sqrt{2}$  are then equal to the constants  $a_{1,m}(t_i)$  in Eqs. (5), where only the triplet states are involved. The factor of  $(\alpha_1\beta_2 - \alpha_2\beta_1)/\sqrt{2}$ , the singlet state, remains unchanged, and is set equal to  $a_{0,0}(t_i')$  in Eq. (6). The eigenvalues and the splittings which result in slow passage are shown by the Zeeman level diagram in Fig. 2. The top and bottom levels (terms in (6a)) are pure triplet states and each of the two closely spaced levels is a linear combination of singlet and triplet states (terms (6b) and (6c)). For  $\delta \rightarrow 0$ ,  $Q=0$  and  $Q_1=\infty$ , and the mixed state with the energy eigenvalue  $E_0'$  now becomes a pure singlet state. The  $J$  splitting therefore disappears because transitions to and from the pure singlet state are forbidden. This supports the fact in the case of two equivalent nuclei that no  $J$  splitting is observed.<sup>15</sup> For  $\delta \sim J$  the intensities of the transitions indicated are determined by the particular transition probabilities between the given states as well as by their statistical weights. In the order of increasing frequency the magnitudes of the absorption lines are in the ratio of

$$\frac{1}{1+Q'^2} : \frac{1}{1+Q^2} : \frac{1}{1+Q^2} : \frac{1}{1+Q'^2}.$$

In the limit  $J \ll \delta$  then  $Q=-1$ ,  $Q'=+1$ , all of the amplitudes are equal, and the  $J$  splittings conform to the rule given by Gutowsky.<sup>15</sup>

The expectation value of the precessing components

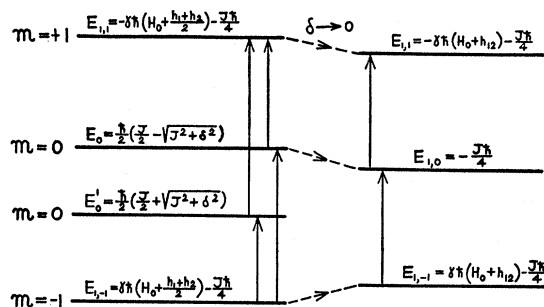


FIG. 2. Zeeman energy level diagram for a nonequivalent two-spin system ( $I=\frac{1}{2}$  for each spin). For  $\delta=0$  the magnitude of  $h_{12}=h_1=h_2$  chosen is arbitrary.

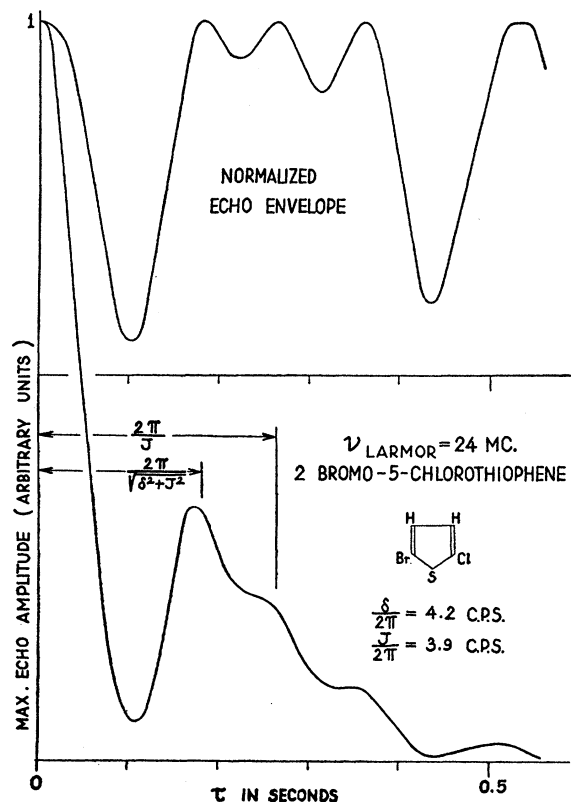


FIG. 3. Experimental echo envelope plots for protons in 2-bromo-5-chlorothiophene. The lower plot of the observed envelope is normalized to unity in the upper plot in order to correct for the damping due to spin relaxation and diffusion. The upper plot refers to the abscissa directly beneath it. Because of thermal diffusion, the damping for this particular measurement is greater than the damping shown for the same compound in Fig. 1. The magnetic field  $H_0$  over the sample for the above measurement happened to be more inhomogeneous than the field over the sample when the plot in Fig. 1 was photographed.

of nuclear magnetization for  $t \gg \tau + t_w$  will be given by

$$V = u + iv = (\psi^* | I_+ | \psi), \quad (7)$$

where the spin operator

$$I_{\pm} = I_x \pm iI_y = I_{x1} + I_{x2} \pm i(I_{y1} + I_{y2})$$

is averaged over  $\psi$  given by (6), and the integral is written in Dirac notation.  $u$  and  $v$  are the observed real and imaginary components of induction, respectively. For the condition that  $H_1$  and  $t_w$  are the same for both pulses, the exact expression for the maximum of the spin echo amplitude, at  $t = 2\tau$ , is given in Appendix A. In the spin echo experiment only the absolute value of (7), given by  $|V|$  at  $t = 2\tau$ , is observed. Only the terms independent of  $H_0$  contribute to the echo at  $t = 2\tau$ , assuming that  $\tau \gg 1/\gamma\Delta H$ , and therefore the free induction signals which follow directly after pulses do not interfere with the echo. We have neglected any damping due to  $T_2$  and thermal diffusion in arriving at this result. The observed spin echo envelope must therefore be normalized and plotted as a function of  $\tau$

in order to compare with theory. This procedure is valid, as we shall point out, providing that both of the coupled nuclei have the same  $T_2$  and that the presence of other neighboring nuclei with finite magnetic moments in the molecule do not effectively couple, in this case, with the two proton system. For example, the influence of the  $\text{Cl}^{35}$ ,  $\text{Cl}^{37}$  moments on the  $J$  coupling between the protons in dichloroacetaldehyde ( $\text{CHCl}_2\text{CHO}$ ) appears to be absent. This can be accounted for by the fact that the quantum states of the chlorine nuclei are short lived due to quadrupole broadening, and thus chlorine has a relaxation time which is small compared to  $T_2$  of the protons and to  $1/J$ . This process is treated later in a special case (Part IV). Thus, any  $J$  coupling that exists between chlorine and hydrogen averages to zero as far as the experiment can detect.

For  $\omega_1 t_w = \pi/2$  the observed and the normalized plots of the envelope due to protons in 2-bromo-5-chlorothiophene<sup>23</sup> are given in Fig. 3. In this case the theoretical expression for the envelope is given by

$$|V| = \frac{M_0 \delta^2}{2(\delta^2 + J^2)} \left| 1 + \frac{J^2}{2\delta^2} - 2 \sin^2(J\tau/2) \sin^2[\tau(J^2 + \delta^2)^{1/2}/2] \right|, \quad (8)$$

which agrees with the normalized plot within experimental error. At a Larmor frequency  $\omega/2\pi = 24$  Mc,  $J/2\pi = 3.9$  cps and  $\delta/2\pi = 4.2$  cps. At  $\omega/2\pi = 32$  Mc,  $\delta/2\pi = 5.6$  cps, and  $J$  remains unchanged. The parameter  $\delta$  appears to be linearly proportional to  $H_0$ , and every case bears out this fact where  $\delta$  can be resolved. For  $\delta \sim J$  in this case, the  $xy$  components of  $J$  coupling cannot be neglected in comparison to the coupling in the  $z$  direction, and the magnetic quantum number  $m$  is not a constant of the motion. In most cases, however, it is observed that  $J \ll \delta$ , and we let  $J\mathbf{I}_1 \cdot \mathbf{I}_2 \rightarrow JI_{1,z}I_{2,z}$ . This is analogous to the approximation made in the Paschen-Back effect, where the large magnetic field in that case plays the role of  $\delta$ . The observed plot has been reported<sup>18</sup> for the echo envelope of protons in dichloroacetaldehyde, giving  $\delta/2\pi = 104$  cps and  $J/2\pi = 2.7$  cps at  $\omega/2\pi = 32$  Mc. The plot agrees with the expression (8) for  $J \ll \delta$ .

One might suspect that the protons in dichloroacetaldehyde do not have just single chemical shifts  $h_1$  and  $h_2$ , but several because of the possible structural isomers of  $\text{CHCl}_2\text{CHO}$ . However, we assume that the rapid transfer between these possible isomers causes an averaging into two definite chemical shifts, one for each proton. This will be shown to result when the lifetimes in each isomeric state (estimated from known chemical barriers which give rise to hindered rotation) are much shorter than  $2\pi/\delta$ .

<sup>23</sup> We wish to thank Professor H. S. Mosher of the Stanford Chemistry Department for a special synthesis of this compound.

III.  $J$  COUPLING AMONG THREE OR MORE SPINS

A generalized form of the  $J$  coupling Hamiltonian among  $n$  spins, given by

$$\mathcal{H} = -\sum_{j=1}^n [\hbar\gamma_j \mathbf{I}_j \cdot (\mathbf{H} + \mathbf{h}_j)] + \frac{1}{2} \sum_{\substack{i=1, \\ i \neq j}}^n \hbar J_{ij} \mathbf{I}_i \cdot \mathbf{I}_j, \quad (9)$$

shall be used to express the coupling, where  $\mathbf{H}$  is an arbitrary external magnetic field and  $\mathbf{h}_j$  is the chemical shift of the  $j$ th nucleus. Consider the coupling of two nonequivalent spin groups  $A$  and  $B$ , where  $K_A$  and  $K_B$  denote the coupling between equivalent spins in groups  $A$  and  $B$ , respectively. The Hamiltonian (9) can then be written as

$$\mathcal{H} = -\gamma\hbar[\mathbf{S}_A \cdot (\mathbf{H} + \mathbf{h}_A) + \mathbf{S}_B \cdot (\mathbf{H} + \mathbf{h}_B)] - \hbar J \mathbf{S}_A \cdot \mathbf{S}_B - C(K_A S_A^2, K_B S_B^2, K_A I_A^2, K_B I_B^2), \quad (10)$$

where

$$\mathbf{S}_A = \sum_{k=1}^{n_A} \mathbf{I}_k, \quad \mathbf{S}_B = \sum_{l=1}^{n_B} \mathbf{I}_l,$$

$\gamma = \gamma_A = \gamma_B$ , and  $I_A$  and  $I_B$  are the spin values of component nuclei in groups  $A$  and  $B$ , respectively.  $C$  is a function of terms, as indicated, which commutes with  $\mathcal{H}$ , and introduces the coefficients  $K_A$  and  $K_B$  as constants in the energy eigenvalues of this system. These coupling constants do not appear in the differences between these eigenvalues, and therefore are not observed in resonance splittings. Of course, if  $\delta = 0$  then  $J$  coupling disappears for the same reason, namely, that  $\mathbf{S}_A \cdot \mathbf{S}_B \rightarrow S_A S_B$ , and a single resonance line results. In the spin echo experiment the interference effect which gives rise to the envelope modulation correspondingly vanishes.

## A. Coupling Among Three Spins

The result for the exact calculation ( $\delta$  and  $J$  arbitrary) in which two equivalent spins couple with a third spin ( $I = \frac{1}{2}$  for each spin and  $\gamma_A = \gamma_B$ ) is given in the Appendix B. In Fig. 4 the observed echo envelope due to three protons in  $\text{CHCl}_2\text{CH}_2\text{Cl}$  is plotted, where  $J/2\pi = 6.0$  cps and  $\delta/2\pi = 48$  cps at  $\omega/2\pi = 24$  Mc. Figure 5 shows photographs of these echoes at 31 Mc. This case also applies to protons in  $\text{CHCl}_2\text{CHClCHCl}_2$ , where  $J/2\pi = 5.3$  cps and  $\delta/2\pi = 38$  cps at  $\omega/2\pi = 24$  Mc. The proton echo envelopes for both of these molecules is accurately described if terms involving only the ratio  $J/\delta$ , taken to the first power, are retained in the exact expression given in Appendix B. The Zeeman energy level diagram is shown in Fig. 6. Schiff<sup>24</sup> describes the symmetry properties of the various spin functions which are linearly combined to give the particular states as indicated. For  $\delta = 0$  the states corresponding to the eigenvalues  $E_3$  and  $E_5$  can only have

<sup>24</sup> L. I. Schiff, *Quantum Mechanics* (McGraw-Hill Book Company, Inc., New York, 1949), p. 229.

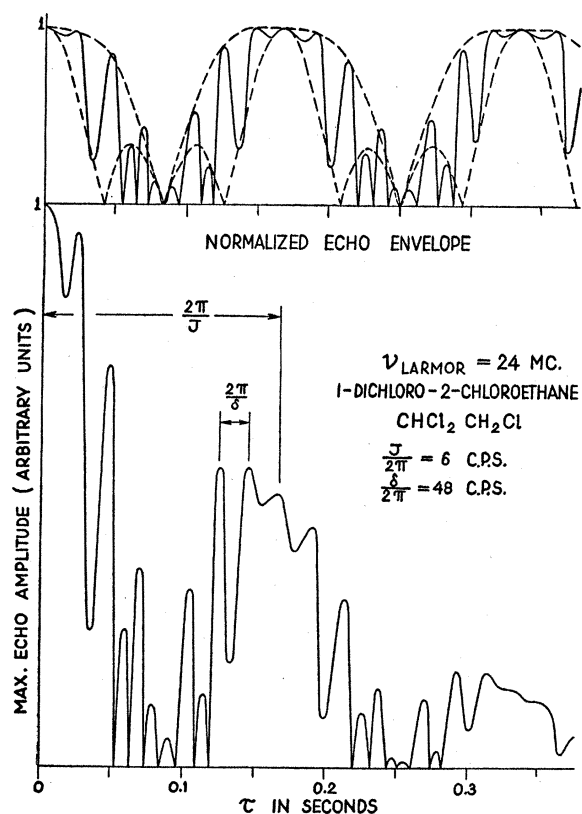


Fig. 4. Experimental echo envelope plots for protons in 1-dichloro-2-chloroethane. The meaning of the lower and upper solid line plots is the same as in Fig. 3. The dotted lines plotted from the theory trace out the envelope of the upper and lower limits of the echo envelope modulation plot. The periodic doubling of the modulation frequency appears because the echo experiment reveals only the absolute magnitude of the echo modulation. The region of modulation doubling (as indicated within the small dotted lobes which meet the abscissa) signifies in the theory that the sinusoidal plot changes sign for a few cycles; that is, with respect to a reference axis, the nuclear magnetization vector of the echo reverses direction by  $180^\circ$ .

transitions between themselves and cannot combine with any other state. All transitions then involve only a single energy difference, and a single resonance absorption line results. Under any circumstance, the coupling between the equivalent protons cannot be observed for reasons which have been discussed in the two proton case.

In the approximation that  $J \ll \delta$ , the relative intensities and the number of lines which result are in accordance with the following empirical rules found by Gutowsky<sup>15</sup> for nuclei with  $I = \frac{1}{2}$ . (a) The resonance of  $n_A$  equivalent spins in group  $A$ , with maximum total spin  $S_A = n_A/2$ , is split into  $2S_B + 1$  equidistant lines by an equivalent spin group with total maximum spin  $S_B$ , and conversely for the resonance of spin group  $B$ . (b) The relative intensities of the resonance lines of  $A$  are determined by the binomial coefficient  $\binom{2S_B}{N_A - 1}$ , which determines the relative amplitude of the  $N_A$ th

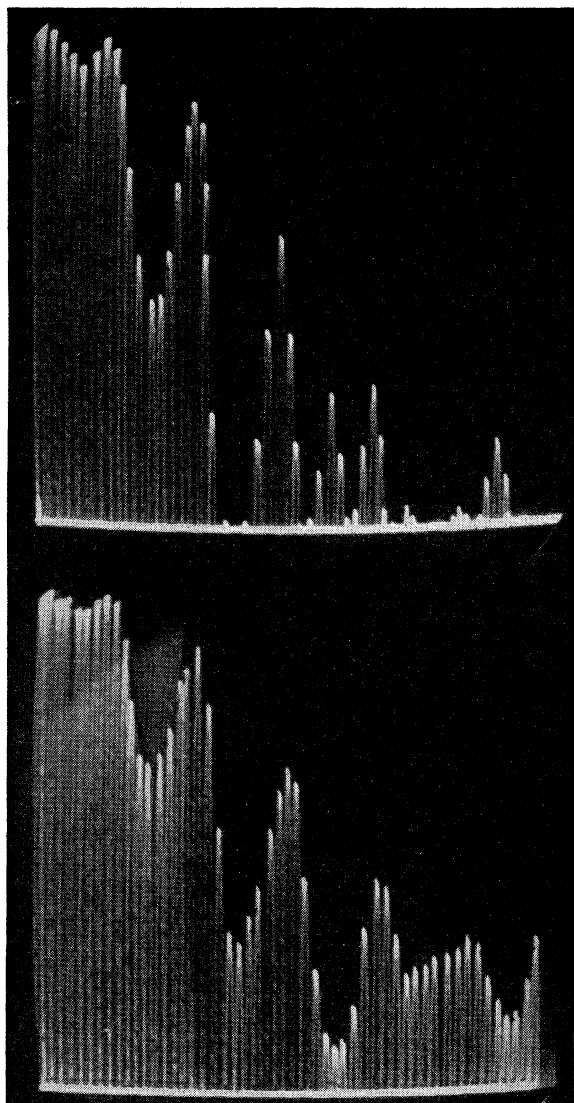


FIG. 5. The upper photograph shows the echo envelope due to protons in pure  $\text{CHCl}_2\text{CH}_2\text{Cl}$  at a Larmor frequency of 31 Mc. Both photographs are obtained by the method indicated in Fig. 1. The time duration of the total sweep is 0.22 sec. The lower photograph shows, on the same time scale as the upper one, the echo envelope due to protons in a mixture of  $\text{CHCl}_2\text{CH}_2\text{Cl}$  and chloroform ( $\text{CHCl}_3$ ). The echo modulation frequency doubling effect, which is seen in the pure compound above, does not appear below because the echo component produced by the protons in  $\text{CHCl}_3$  (which alone does not exhibit envelope modulation) serves as reference upon which the sinusoidal echo modulation due to  $\text{CHCl}_2\text{CH}_2\text{Cl}$  may superimpose. Thus, the total echo vector never reverses direction (see caption of Fig. 4).

line ( $N_A = 1, \dots, 2S_B + 1$ ). (c) In addition, the ratio of the splitting, measured in gauss, between adjacent lines of group  $A$  to that in group  $B$  is given by  $\mu_B I_A / \mu_A I_B$ .<sup>25</sup> However, in cases where  $\delta \sim J$  the above rules break down. In Fig. 6 more than  $2(S_A + S_B + 1) = 5$  lines appear in this case.

<sup>25</sup> Although rule (b) holds only for  $I = \frac{1}{2}$ , rules (a) and (c) hold for arbitrary  $I$ , where  $S = nI$  replaces  $S = n/2$ .

### B. Generalization of the Coupling for $J \ll \delta$

In most of the observed cases it is found that  $J \ll \delta$ , and the Hamiltonian (10) in the absence of  $H_1$  can be written as

$$\mathcal{H} = -\gamma \hbar [S_{z,A}(H_0 + h_A) + S_{z,B}(H_0 + h_B)] - \hbar J S_{z,A} S_{z,B}. \quad (11)$$

The average of the  $x$  and  $y$  components of  $J$  coupling over the period  $2\pi/\delta$  is negligible compared to the coupling in the  $z$  direction. The rule given for the number and intensities of the lines may be understood, for example, if we consider that spin group  $A$  sees a local magnetic field given by  $H_0(A) = H_0 + h_A + J S_{z,B}/\gamma$  and conversely for group  $B$ . There are  $2S_B + 1$  possible values of  $S_{z,B}$ , where each of these values has the statistical weight given by the number of ways in which the component spins of a group may be oriented in order to provide a given  $S_z$ . For  $I = \frac{1}{2}$  this statistical weight is given by the binomial coefficient presented previously, where  $N_A - 1 = S_B + S_{z,B}$  and  $S_{z,B} = S_B, S_B - 1, \dots, -S_B$ .

With the above approximation in mind, consider a physical model of the echo modulation in which the local magnetic  $J$  field due to the  $z$  component of a macroscopic spin vector  $\mathbf{M}_A$  is seen by  $\mathbf{M}_B$  and vice versa (let  $M_A$  and  $M_B$ ). If both of these vectors precess with precisely the same Larmor frequencies, which is to say that  $\delta = 0$ , it becomes impossible by means of rf absorption to cause the  $z$  magnetic fields due to  $J$ , seen by both vectors, to differ. In the more precise terms of the quantum-mechanical calculation, a constant  $J$  term is added to all of the energy eigenvalues of the coupled system, and  $J$  does not appear in the differences between those eigenvalues of spin states involved in allowed transitions. However, if  $\delta$  is finite, a vector model will show how the difference in Larmor precession frequencies makes it possible for  $\mathbf{M}_A$  and  $\mathbf{M}_B$  to interfere with each other due to  $J$  coupling. Let both of these vectors precess in the  $xy$  plane after the first pulse (let  $\omega t_w = \pi/2$ ) and view the system from  $xy$  coordinates which precess at the Larmor frequency of  $\mathbf{M}_A$ . Since  $M_{z,A} = M_{z,B}$  after the first pulse (which is true regardless of the value of  $\omega t_w$  under the conditions of the experiment), the only difference in Larmor precession frequency between these vectors during the time between  $t_w$  and  $\tau$  is that due to the chemical shift. At the time a second rf pulse is turned on at  $t = \tau$ , then  $M_{xy,A}$  and  $M_{xy,B}$  are out of phase by  $\delta\tau$  radians. After the second pulse rotates the  $\mathbf{M}$  vectors 90 degrees in their respective cones,<sup>14</sup> the difference

$$M_{z,A}(\tau + t_w) - M_{z,B}(\tau + t_w) = M_A - M_B \cos \delta\tau.$$

Now, following the time  $t = t_w + \tau$ , the  $\mathbf{M}$  vectors precess freely with a difference in Larmor frequency given by the chemical shift  $\delta$  plus a difference in frequency due to the  $J$  coupling  $z$  field; the vectors  $\mathbf{M}_A$  and  $\mathbf{M}_B$  do not precess in equal fields due to  $J$  because  $M_{z,A} \neq M_{z,B}$ . According to our model, this frequency difference is



proportional to the difference in  $M_z$  between the two vectors after the second pulse. Consequently the echoes formed at  $t=2\tau$  by each of the spin groups, represented by the vectors  $\mathbf{M}_A$  and  $\mathbf{M}_B$ , will get out of phase with each other. The magnitude of the resultant formed by these component echoes will depend upon the difference  $M_{z,A}(\tau+t_w) - M_{z,B}(\tau+t_w)$ , which determines the extent to which  $\mathbf{M}_A$  and  $\mathbf{M}_B$  precess in different local fields after the second pulse. As  $\tau$  is increased, the phase difference at  $t=2\tau$  between  $M_{xy,A}$  and  $M_{xy,B}$  varies sinusoidally, the maximum echo amplitude therefore varies sinusoidally, and the echo envelope modulation will contain frequencies which depend upon  $J$  and  $\delta$ . If  $J=0$ , on echo modulation cannot appear because the phase difference between  $M_{xy,A}$  and  $M_{xy,B}$  due to  $\delta$ , which is accumulated before the second pulse, is exactly reversed or neutralized at the time the echo is formed. If  $\delta=0$ , no accumulated frequency difference may arise due to  $J$  coupling, although the coupling still exists, because  $M_{z,A}$  is always equal to  $M_{z,B}$ . This model also explains why no echo modulation is observed for one equivalent spin group at resonance which is coupled to another spin group off resonance. It is obvious that both nonequivalent spin groups ( $\mathbf{M}_A$  and  $\mathbf{M}_B$ ) must be flipped by rf pulses in order that they may interfere with each other in a sinusoidal manner. It must be kept in mind that this macroscopic model does not give the correct quantitative expression given by Eq. (8), derived quantum-mechanically.

A generalized method for calculating the spin echo due to two nonequivalent groups which couple is now presented. The Hamiltonian (11) has the useful properties (1) that the magnitudes of the total spins  $S = |S_{\max}|$ ,  $|S_{\max}-1|$ ,  $|S_{\max}-2|$ ,  $\dots$  of each group are constants of the motion, and (2) that the  $S_z$  operators are good quantum numbers in the approximation that  $J \ll \delta$ . For each group with a given  $S$ , providing that  $\delta t_w \ll 1$ , the probability amplitudes  $a_{m,S}$  are transformed to  $a_{m',S}$  (by an rf pulse) by the function

$$T_{S,m,m'} = [(S+m)!(S-m)!(S+m')!(S-m')!]^{\frac{1}{2}} \times i^{2S-m-m'} \sin^{2S}(\omega_1 t_w/2) \sum_{\rho=0}^{\infty} (-1)^{\rho} \times \frac{\cot^{m+m'+2\rho}(\omega_1 t_w/2)}{(m+m'+\rho)!(S-m'-\rho)!(S-m-\rho)! \rho!}, \quad (12)$$

given by Bloch and Rabi.<sup>21</sup> The terms in the sum over  $\rho$  are suppressed for any factorial of a negative integer which appears in the denominator, since the factorial is then infinite. For two rf pulses applied to the spin ensemble, which is initially at thermal equilibrium, the

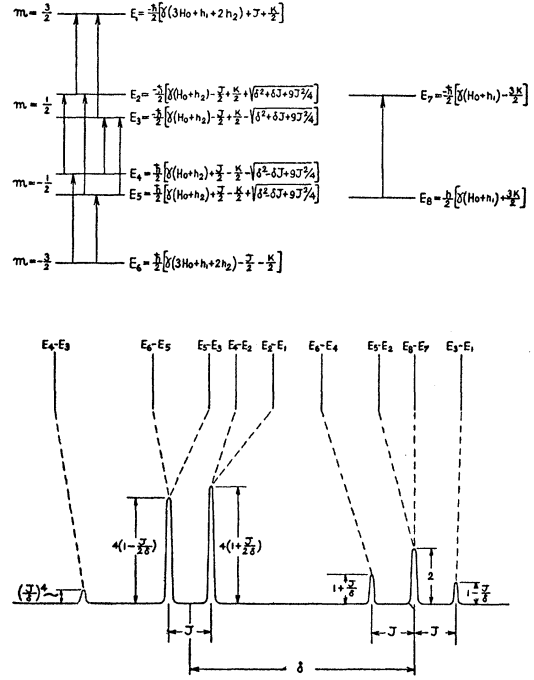


FIG. 6. Zeeman energy level diagram for a three spin system with  $S_A=1$ ,  $S_B=\frac{1}{2}$ ,  $I_A=I_B=\frac{1}{2}$ . The solid vertical lines indicate the number and arbitrary spacing of the resonance transitions which would be observed in the steady state for  $J \sim \delta$ . The dotted lines show how these lines relate to the resonance lines at the bottom for the condition that  $J < \delta$ .

spin wave function at  $t=2\tau$  is given by

$$\psi(2\tau) = \sum_{\substack{S_A, S_B, m_A, m_B, \\ m_A', m_B', m_A'', m_B''}} \{ \phi_{S_A, m_A'} \phi_{S_B, m_B''} T_{S_A, m_A', m_A''} \times T_{S_B, m_B', m_B''} T_{S_A, m_A, m_A'} T_{S_B, m_B, m_B'} \times a_{S_A, m_A}(0) a_{S_B, m_B}(0) \exp -i\tau[\gamma(H_0+h_A) \times (m_A'+m_A'') + \gamma(H_0+h_B)(m_B'+m_B'') + J(m_A'm_B'+m_A''m_B'')] \}, \quad (13)$$

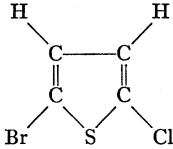
where

$$\sum_{S_A, m_A} |a_{S_A, m_A}(0)|^2 + \sum_{S_B, m_B} |a_{S_B, m_B}(0)|^2 = 1.$$

The eightfold sum indicates that each of the two spin groups  $A$  and  $B$  are separately summed over  $S$  and that the probability amplitudes for each group are transformed twice by two rf pulses. The component wave functions characterized by  $m$  are transformed as follows: for the first pulse, ending at  $t=t_w$ ,  $m \rightarrow m'$ , and  $m'$  remains constant for  $t_w \leq t \leq \tau$ ; after the second pulse ending at  $t=\tau+t_w$ ,  $m' \rightarrow m''$ , and  $m''$  is constant for  $t \geq \tau+t_w$ . The arrow indicates that the final state is built up from a superposition of initial  $m$  states. The pulse duration time  $t_w$  is neglected in the exponent since  $t_w \ll \tau$ , but appears in the  $T$  functions. The maximum of the echo at  $t=2\tau$  is determined by calculating the expectation value of the  $I_+$  operator with Eq. (13),



TABLE I. Echo modulation data at  $\nu_{\text{Larmor}}=32$  Mc.

Compound	$J/2\pi$ in cps*	$\delta/2\pi$ in cps*	Figure	Appendix
CHCl <sub>2</sub> CHO	2.7	104	2, 7	A
CH <sub>2</sub> CICHCl <sub>2</sub>	6.0	64	4, 5, 6, 8	B
CHCl <sub>2</sub> CHClCHCl <sub>2</sub>	5.3	51	6, 8	B
CH <sub>3</sub> OH (anhydrous, at -78°C)	5.0	79	9, 17	C-2
CH <sub>3</sub> CHBr <sub>2</sub>	6.3	108	9	C-2
CH <sub>3</sub> CH <sub>2</sub> COOCCl <sub>3</sub>	7.1	94	11, 13	C-3
CH <sub>3</sub> CH <sub>2</sub> OH	7.5	80	compares approx- imately to 11, 13	compares approx- imately to C-3
	3.9	5.6	1, 2, 3	A

\* Estimated error of all data is  $\pm 5$  percent.

using the procedure which led to the expectation value given by (8). The observed echo can be considered as a superposition of echoes from groups *A* and *B*. Each group in turn is a superposition of echoes due to the invariant total spins  $S_A$  and  $S_B$ , respectively. Therefore

$$u + iv = \sum_{S_A} (\psi^* | I_{+,A} | \psi) + \sum_{S_B} (\psi^* | I_{+,B} | \psi), \quad (14)$$

and the matrix elements of  $I_+$ ,  $I_-$ , and  $I_z$  are given by

$$\begin{aligned} \langle m | I_+ | m-1 \rangle &= [(S+m)(S-m+1)]^{\frac{1}{2}}, \\ \langle m | I_- | m+1 \rangle &= [(S-m)(S+m+1)]^{\frac{1}{2}}, \\ \langle m | I_z | m \rangle &= m, \end{aligned} \quad (15)$$

where  $\Delta S_A, \Delta S_B = 0$ ;  $|\Delta m_A| = 1, \Delta m_B = 0$ ;  $|\Delta m_B| = 1, \Delta m_A = 0$ . After the operation is performed in Eq. (14) it is necessary to collect common factors of the term  $|a(0)_{S,m}|^2$  and relate them to  $M_0$ , the macroscopic equilibrium magnetization. This is done by using the following relations:

$$\begin{aligned} M_0 &= \sum_{S_A} \sum_{S_B} (2S_B + 1) \sum_{m_A} m_A |a_{S_A, m_A}(0)|^2 \\ &\quad + (2S_A + 1) \sum_{m_B} m_B |a_{S_B, m_B}(0)|^2, \\ (2S_{B,A} + 1) \sum_{m_{A,B}} m_{A,B} |a_{S_A, B, m_{A,B}}(0)|^2 \\ &= M_0 F_{A,B} / \sum_{S_A} \sum_{S_B} F_{A,B}, \end{aligned} \quad (16)$$

where

$$F_{A,B} = (2S_{B,A} + 1)(S_{A,B})(S_{A,B} + 1)(2S_{A,B} + 1).$$

The above treatment can apply to more than two spin groups which couple, and the number and type of rf pulses (characterized by  $t_w$  and  $H_1$ ) may be arbitrary. Both of the spin groups *A* and *B* for most of our experiments are taken to be at the nuclear resonance condition during the application of pulses because of the condition

$\omega_1 \gg \gamma \Delta H, \delta, J$ . We have treated several cases involving three spin groups (Appendix C-5, C-6) in which two are at resonance and the third group is not at resonance.<sup>26</sup> The group off resonance, such as  $F^{19}$ , usually has a gyromagnetic ratio sufficiently different from the nuclei at resonance, such as protons, so that  $(\gamma_F - \gamma_H)H_0 \gg \omega_1$ . The modifications required of the above calculations are obvious in these cases and we shall not discuss them here. Experimental values of  $J/2\pi$  and  $\delta/2\pi$  are given in Table I for typical cases. The experimental echo plots for these cases are in agreement within experimental error with the theoretical plots. Particular references to formulas in the appendix and to figures are given in this table.

#### IV. DAMPING OF THE $J$ COUPLING

For most of the cases which exhibit echo modulation it is found that the entire envelope decays with a lifetime determined by  $T_2$  and thermal diffusion. The observed envelope is normalized to unity and agreement is obtained with the above theory, in which the  $J$  coupling is assumed to be undamped or uninterrupted. However, it is possible that the  $J$  coupling may be perturbed not only because of  $T_2$ , but also because of certain effects such as rotational hindrance (discussed in II with respect to CHCl<sub>2</sub>CHO) and molecular dissociation. In all of these cases the phase coherence of the spin ensemble, which must be maintained in order to observe the  $J$  coupling, is destroyed to some extent because of the random interruption of the magnetic coupling between neighboring nuclei. The mechanisms

<sup>26</sup> We have discovered in the liquid compounds CFCIHCHCl<sub>2</sub> and CF<sub>2</sub>HCHCl<sub>2</sub> (which were reasonably pure) that fluorine echoes exhibit modulation and that there is a main splitting ( $\sim 1$  kc at  $\omega/2\pi = 30$  Mc) of the fluorine resonance into two lines which is proportional to  $H_0$ . This is unexpected because (1) equivalent nuclei alone cannot exhibit a field dependent splitting which is due to the chemical shift, and (2) there can be no echo modulation from equivalent nuclei at resonance unless they are coupled to a second group of nuclei which is also at resonance and is nonequivalent with respect to the first group. In the molecules above, anomalous signals are obtained from fluorine nuclei which are coupled to two neighboring protons which are not at the echo resonance and which are nonequivalent among themselves. However, fluorine echoes do not show a modulation (nor is there a field dependent splitting of the fluorine resonance) in similar molecules where equivalent fluorine nuclei are neighbors of protons which are equivalent among themselves. We suggest, therefore, that the anomalous fluorine signals are due to the  $J_{FH}$  coupling of fluorine with the nonequivalent protons, and that the anomaly will be particularly strong if  $J_{HH} \sim \delta_{HH}$  for the protons. In this event the  $xy$  component of  $J_{HH}$  coupling (which derives from the term  $[I_{x1} + I_{x2} + i(I_{y1} + I_{y2})]J_{HH}$ ) is sufficiently strong to cause the protons to flip each other at a rate which may be comparable to the inverse of the lifetime of the fluorine echo envelope. Consequently the  $J_{FH}$  coupling between the protons and fluorine will be modulated by the change in proton spin orientation. In turn the local field at the fluorine nucleus (due to  $J_{FH}$  coupling) will be modulated at the rate at which the protons are flipping. This modulation, together with the magnitude of  $J_{FH}$ , determines the magnitude of the fluorine resonance splitting and echo modulation. The frequency of the echo modulation is not related to the fluorine resonance splitting, and, in fact, is field independent. We shall not attempt here to account for this characteristic of the echo modulation, but the above argument thus far does account for the fact that the fluorine resonance splitting should depend on the ratio  $\delta_{HH}/J_{HH}$ , and therefore on the field  $H_0$  (since  $\delta_{HH} \propto H_0$ ).

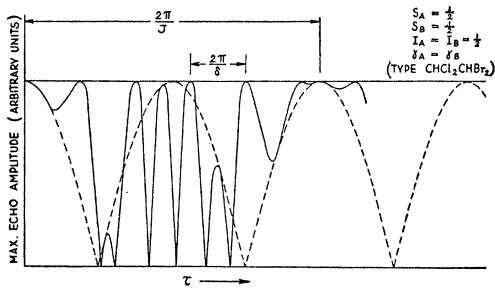


FIG. 7.

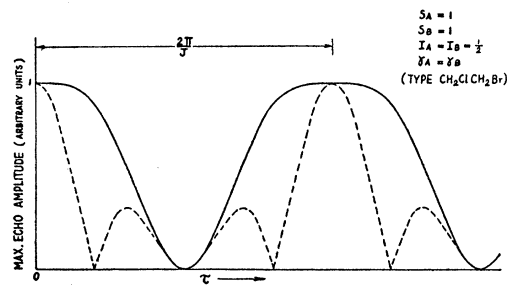


FIG. 10.

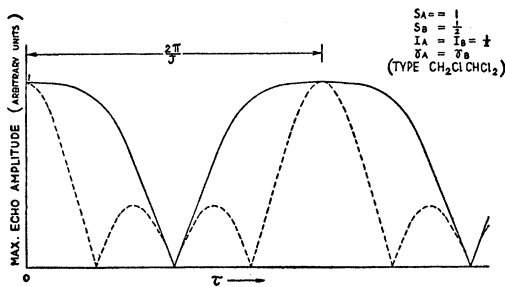


FIG. 8.

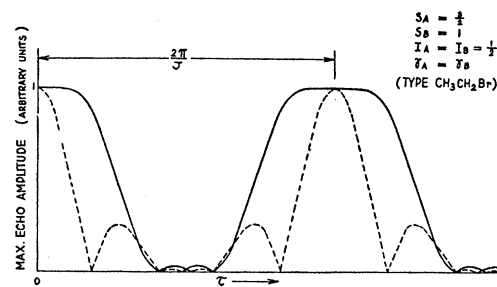


FIG. 11.

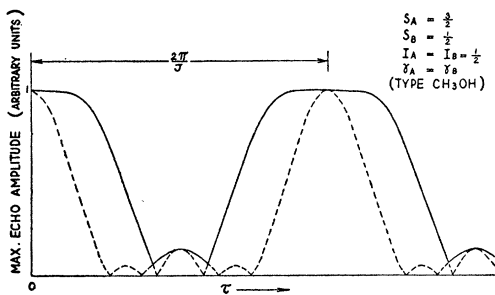


FIG. 9.

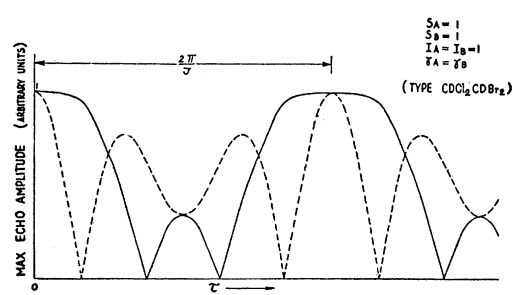


FIG. 12.

Figs. 7-12. For the condition  $J \ll \delta$ , theoretical plots for various spin systems (obtained from formulas in the appendix) are shown which trace out the upper and lower limits of the echo envelope modulation. These traces are periodic with frequency  $J/2\pi$ . The echo envelope, modulated at a higher frequency  $\delta/2\pi$ , may be fitted and plotted within the solid and dotted lines, as shown in Figs. 4 and 7. Frequency doubling occurs within the first dotted lobes which meet the axis symmetrically in time, and the doubling reappears periodically.

by which this random process takes place shall be described (1) by letting  $\delta$  and  $J$  take on different discrete values ( $m$  constant in the absence of  $H_1$ ) in order to describe such effects as the transfer between rotational molecular isomers, and (2) by letting the quantum state  $m$  change to other allowed  $m$  states in a random manner ( $J$  and  $\delta$  constant) in order to describe the effect of  $T_1$  and  $T_2$ .

### A. Damping by Fluctuations of $J$ and $\delta$

First let us treat the damping process of the case previously treated by the Hamiltonian (1) above. Assume for a given orientation of two coupled nuclear moments in a molecule that a certain  $J$  and  $\delta$  can be assigned to the system. During the time the molecule exists in an alternate form the coupled nuclei are described by the parameters  $J'$  and  $\delta'$ . By the method

given in III the expectation value of  $I_+$  after the first rf pulse is given by

$$V = \frac{iM_0}{4} \left\{ \exp i[\gamma(H_0 + h_1) + J/2]t + \exp i[\gamma(H_0 + h_1) - J/2]t + \exp i[\gamma(H_0 + h_2) + J/2]t + \exp i[\gamma(H_0 + h_2) - J/2]t \right\} = \sum_{n=1}^4 f_n, \quad (17)$$

where  $I = \frac{1}{2}$ ,  $J \ll \delta$ ;  $h_1, h_2 \rightarrow h'_1, h'_2$ , and  $J \rightarrow J'$  for the other structure. Each of the two states of the molecule will have a lifetime given by  $(\lambda)^{-1}$  and  $(\lambda')^{-1}$ . The term  $f_n$  (where  $n = 1, \dots, 4$ , in this case) represents the  $n$ th component of  $n$  terms, each characterized by frequency  $\omega_n$ , which add to give the macroscopic transverse

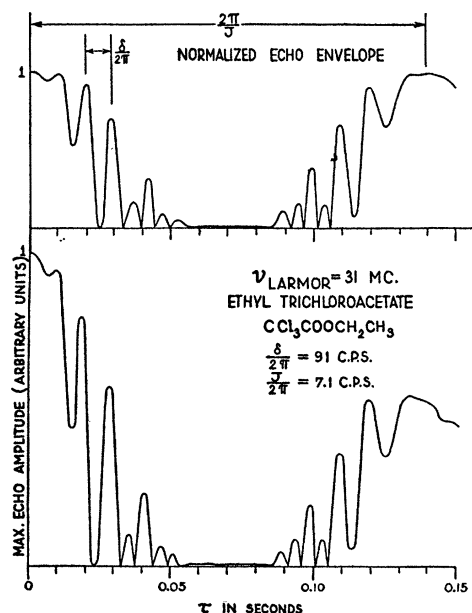


FIG. 13. Experimental echo modulation plot due to protons in ethyl trichloroacetate. See Fig. 3 for meaning of both plots.

nuclear magnetization after the first rf pulse. The interchange of the  $h$  and  $J$  parameters ( $h_1, h_2 \rightleftharpoons h'_1, h'_2$ ;  $J \rightleftharpoons J'$ ) requires that the expectation value given by Eq. (17) be corrected in order to account for the damping which will result because of incoherence. The phenomenological equations of coupling which we use to account for the damping are as follows:

$$\begin{aligned} \dot{F}_n - i\omega_n F_n &= -\lambda F_n + \lambda' F'_n, \\ \dot{F}'_n - i\omega'_n F'_n &= -\lambda' F'_n + \lambda F_n. \end{aligned} \quad (18)$$

The solutions for  $F_n$  are now the corrected values which include the damping and replace  $f_n$  in Eq. (17). For our particular case there are four pairs of equations of this type, one set for  $F_n$  and another set for  $F'_n$ . In order to obtain the echo at  $t = 2\tau$  it is again convenient to calculate  $\mu + i\nu$  for  $t \geq \tau + t_w$  with no damping. The result is

$$V = \frac{-i}{M_0} \sum_{k=1}^4 [f_k(t) \sum_{n=1}^4 f_n^*(\tau) (1 - 2\delta_{k, 5-n})], \quad (19)$$

where  $f_n^*(\tau)$  is the complex conjugate of  $f_n(\tau)$ , and  $\delta_{k, 5-n}$ , the Kronecker delta, is zero for  $k \neq 5-n$  and unity for  $k = 5-n$ . Each product of  $f_k(t)$  and the sum of four constant  $f_n(\tau)$  terms is one of four such product terms, each characterized by frequency  $\omega_k$ , which sum to give the solution for  $V = u + i\nu$  after the second pulse. Now all of the  $f$  terms of Eq. (19) must be corrected for damping. The corrected solutions  $F_n(\tau)$  of Eq. (18) replace  $f_n(\tau)$  in the expression for  $V$  in Eq. (19). A new set of equations, analogous to the set given by Eq. (18), is then solved for the corrected  $F_k$  terms, and these terms replace the  $f_k(t)$  terms in Eq. (19). Two sets of such equations, one for the prime and one for the

unprime system, form two solutions  $V_1$  and  $V_2$  for the echo expression given by Eq. (19), and the observed echo is given by  $V = V_1 + V_2$ .  $V$  is obtained for the following conditions:

$$(\lambda, \lambda' \ll \delta, \delta', J, J')$$

$$|V| = \frac{1}{2} M_0 |1 - 2 \sin^2(\delta_a \tau / 2) \sin^2(J_a \tau / 2)|, \quad (20a)$$

where

$$\delta_a = (\lambda \delta' + \lambda' \delta) / (\lambda + \lambda') \quad \text{and} \quad J_a = (\lambda J' + \lambda' J) / (\lambda + \lambda');$$

$(\lambda, \lambda' \ll \delta, \delta', J, J')$ :

$$\begin{aligned} |V| = \frac{M_0}{2(\lambda + \lambda')} & \left| \lambda' \left( 1 - 2 \sin^2 \frac{\delta \tau}{2} \sin^2 \frac{J \tau}{2} \right) \right. \\ & \left. + \lambda \left( 1 - 2 \sin^2 \frac{\delta' \tau}{2} \sin^2 \frac{J' \tau}{2} \right) \right|. \end{aligned} \quad (20b)$$

The above calculation can be generalized to apply to any case, and appears to be useful for the analysis of observable rate processes which cause a change in the chemical environment of the nucleus.<sup>27</sup> We see from Eq. (20a) that a fast interchange between different values of  $J$  and  $h$  results in the observation of average values of these parameters, and justifies our assumption that  $J$  and  $h$  are averaged over all possible rotational isomers of the ethyl type compounds which we have investigated. No echoes have been observed in which case Eq. (20b) above applies. We shall not give the general solution for the damping of  $V$ , which can be obtained from Eq. (19). In Appendix D the random process for the above case of damping, which is described by the phenomenological equations of Eq. (18), is treated by a Fourier analysis and shown to lead to the same result which is obtained by the use of Eq. (18).

### B. Effect of Relaxation Time on the Echo Envelope

The damping effect due to relaxation is treated by considering the random change of the quantum state  $m$ . Let us use a model in which two nuclei with  $I = \frac{1}{2}$  have different relaxation times, and are coupled by  $J$  under the conditions which led to the result given by (8), except that we let  $J \ll \delta$ . Assume, as  $t$  increases after the first pulse, that the states described by  $m_A$  and  $m_B$ , which are initially established after the first pulse, may undergo the possible transformations indicated by the schemes (1)  $m_A \rightleftharpoons -m_A$ ,  $\Delta m_B = 0$ , (2)  $m_B \rightleftharpoons -m_B$ ,  $\Delta m_A = 0$ , and (3)  $m_A \rightleftharpoons -m_A$ ,  $m_B \rightleftharpoons -m_B$ ,  $\Delta(m_A + m_B) = 0$ , where  $m = \frac{1}{2}$ . Each of these three schemes is specified by different relaxation times  $(\lambda_1)^{-1}$ ,  $(\lambda_2)^{-1}$ , and  $(\lambda_3)^{-1}$ .

<sup>27</sup> J. T. Arnold and M. E. Packard, J. Chem. Phys. **19**, 1608 (1951), have found for protons in the OH and CH<sub>3</sub> groups in CH<sub>3</sub>OH and C<sub>2</sub>H<sub>5</sub>OH that  $\delta$  varies with temperature and concentration of several dissolved substances. This may be interpreted as a variation in  $\lambda$  and  $\lambda'$  for the associated and dissociated states of the OH group [U. Liddel and N. F. Ramsey, J. Chem. Phys. **19**, 1608 (1951)].

Schemes (1) and (2) represent the effect of  $T_1$  and mutual spin-spin flipping between nuclei of different molecules. Scheme (3) represents the effect of mutual spin-spin flipping between the coupled spins in the same molecule, where the states  $m_A$  and  $m_B$  change simultaneously. Consider only the damping effect on the  $J$  coupling due to schemes (1) and (2), and assume that the effect due to (3) is negligibly small. The changes in the sign of  $m$  for these schemes are made in the wave function given by (13), and the expectation value of the  $I_+$  operator is calculated for the initial unrelaxed state and each of the two states into which the system can relax. Component  $f$  terms from each of the expectation values are again coupled by equations of the form given in Eq. (18). Each  $f$  term is again characterized by a frequency as in the damping calculation discussed in Part IV. A term  $f$  can be correlated with the corresponding  $f'$  by noting that both of these terms will have a common initial condition factor which is established after the first rf pulse. The solution, including the damping of the echo envelope, is then obtained in the same manner by which the damping in the previous case was calculated (Eq. (20)).  $V$  is obtained for the following conditions:

$$(1/T_2, 1/T_2' \gg J):$$

$$|V| = \frac{1}{4} M_0 (e^{-\theta/T_2} + e^{-\theta/T_2'}), \quad (21a)$$

$$(1/T_2, 1/T_2' \ll J):$$

$$\begin{aligned} |V| &= \frac{1}{4} M_0 e^{-\frac{1}{2}\theta(1/T_2 + 1/T_2')} | (e^{-\theta/2T_2} + e^{-\theta/2T_2'}) \cos^2(J\tau/2) \\ &\quad + 2e^{-\frac{1}{2}\theta(1/T_2 + 1/T_2')} \cos\delta\tau \sin^2(J\tau/2) | \\ &= \frac{1}{2} M_0 e^{-3\theta/2T_2} | 1 - 2 \sin^2(\delta\tau/2) \sin^2(J\tau/2) | \\ &\quad \text{for } T_2 = T_2'; \quad (21b) \end{aligned}$$

$$(1/T_2 > J \gg 1/T_2'):$$

$$|V| = \frac{1}{4} M_0 | \exp(-J^2\theta T_2/4) + e^{-\theta/T_2} \cos^2(J\tau/2) |; \quad (21c)$$

where  $1/2\lambda_1 = T_2$ ,  $1/2\lambda_2 = T_2'$ ,  $\theta = 2\tau$ , and no restrictions are imposed on  $\delta$  except that  $J \ll \delta$ . In Eq. (21a) the echo envelope is damped exponentially, and no modulation appears. The exponent  $3\theta/2T_2$  in Eq. (21b) indicates that an additional relaxation mechanism is present. It arises from the fact that the flipping of one nucleus interrupts the local field due to  $J$  seen by the other nucleus. In the approximation that  $J \ll \delta$  this effect reduces the coherence of precession of the system by contributing a relaxation time of  $T_2/2$  to the exponent. For  $J \sim \delta$  this relaxation time is a function of  $J$  and  $\delta$ , and Eq. (21b) becomes a very complicated expression which will not be given here. The condition expressed by Eq. (21c) shows how the  $J$  coupling is severely damped by a very short relaxation time of one of two coupled nuclei. Although both nuclei in this model are at the resonance condition, the same damping effect applies for one of the nuclei off resonance. This justifies the assumption in cases such as  $\text{CHCl}_2\text{CHO}$ ,

that the coupling due to the chlorine nuclei is absent for small values of  $T_2$  due to quadrupole broadening.

### C. Damping of the Proton Coupling in $\text{CH}_3\text{OH}$

It is observed that the echo modulation due to coupled protons in pure  $\text{CH}_3\text{OH}$  (see Figs. 14-17) is damped when a very small percentage of water is added. Aside from the dissociation effect<sup>27</sup> in  $\text{CH}_3\text{OH}$ , a direct interchange of protons takes place between  $\text{H}_2\text{O}$  and  $\text{CH}_3\text{OH}$  molecules.<sup>28</sup> Ignore the contribution of the dissociation effect to the damping, and assume that the damping is due entirely to the random change of  $m$ , the spin state of the proton in the OH group of  $\text{CH}_3\text{OH}$  introduced by protons transferred from  $\text{H}_2\text{O}$  molecules. Let  $\lambda$  represent the reciprocal of the lifetime of a proton with a given  $m$  state in the OH group of  $\text{CH}_3\text{OH}$ . The echo signal from the small amount of  $\text{H}_2\text{O}$  may be neglected. The result for the echo envelope due to  $\text{CH}_3\text{OH}$ , including the damping, is given for these cases:

$$(\lambda \gg J):$$

$$|V| = (M_0/28) | 3 + 11e^{-4\lambda\tau} \cos^2(J\tau/2) |, \quad (22a)$$

$$(\lambda \ll J):$$

$$\begin{aligned} |V| &= (M_0/112) | e^{-2\lambda\tau} [(11/2) \cos J\tau + 6 \cos^2 J\tau \\ &\quad + \frac{1}{2} \cos 3J\tau] + e^{-3\lambda\tau} [4(2 + \cos J\tau) \\ &\quad - 12 \cos 2J\tau] \cos \delta\tau + 44e^{-4\lambda\tau} \cos^2(J\tau/2) |, \quad (22b) \end{aligned}$$

where no restrictions are imposed on  $\delta$  except that  $J \ll \delta$ . It appears from Figs. 14-17 that dissociation as well as proton exchange is effective in damping the echo envelope. As the concentration of  $\text{H}_2\text{O}$  is increased,  $\delta$  decreases, which is considered to be chiefly caused by the dissociation effect.<sup>27</sup> We shall omit a discussion of the damping calculations for  $\text{CH}_3\text{OH}$  in the case of dissociation, where  $\delta$  and  $J$  fluctuate. The results are very similar to the form of Eqs. (20). On the basis of proton exchange we estimate  $\lambda \sim 1 \text{ sec}^{-1}$  ( $\lambda \ll J, \delta$ ) for a mixture of  $\sim 1$  percent by weight of water at a temperature of  $-4^\circ\text{C}$ .

### V. ORIGIN OF THE $J$ COUPLING

Ramsey and Purcell<sup>29</sup> have suggested that the  $J$  coupling derives mainly from a nuclear-electron-nuclear spin interaction. Gutowsky, McCall, and Slichter<sup>17</sup> have extended their treatment of the coupling in the HD molecule to the coupling between pairs of coupled spin groups in more complicated molecules, and thus account for their observed  $J$  values. We shall not treat this coupling mechanism in detail here, nor attempt to correlate measured  $J$  values with theoretical values,

<sup>28</sup> Many compounds with ionizable hydrogen, such as  $\text{NH}_4\text{OH}$  and  $\text{CH}_3\text{COOH}$ , exchange protons with  $\text{CH}_3\text{OH}$  and damp the echo envelope. For references and a general discussion of proton exchange, see N. V. Sidgwick, *Chemical Elements and their Compounds* (Clarendon Press, Oxford, 1950, Vol. 1, Chapter 1).

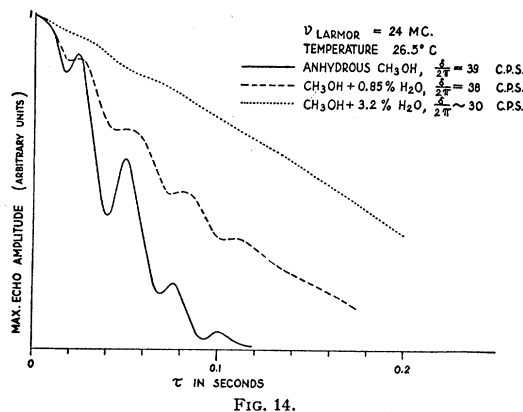


FIG. 14.

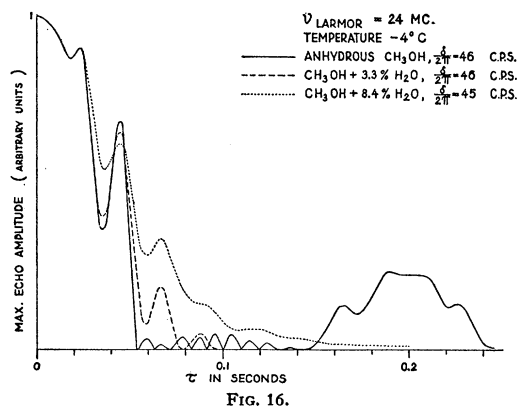


FIG. 16.

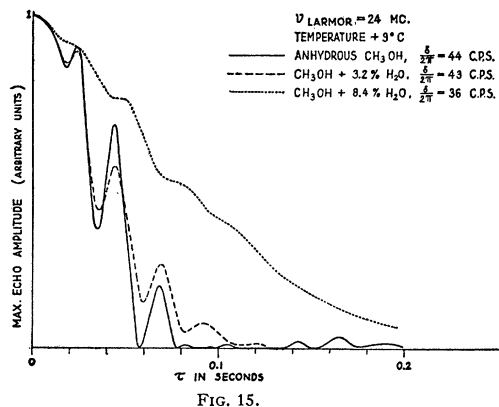


FIG. 15.

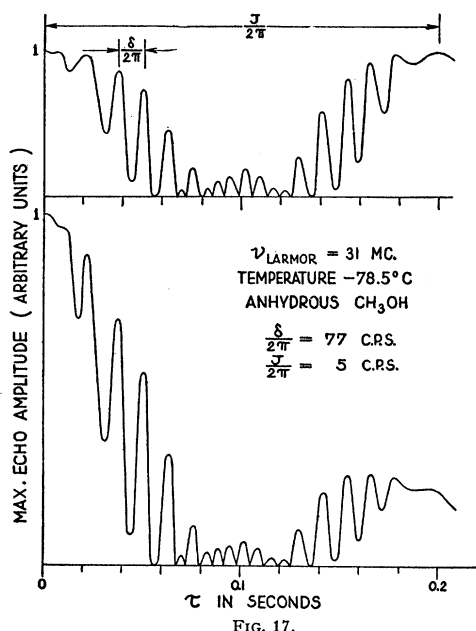


FIG. 17.

FIGS. 14-17. Proton echo envelope plots in methyl alcohol for various temperatures and concentrations of water (expressed in percentage by weight).

but refer the reader to the very adequate discussions of the above authors.

In addition to the spin coupling mechanism there are other mechanisms which give rise to the  $J$  coupling operator, but only account for magnitudes of  $J$  of the order of 1 cps or less. The Hamiltonian which describes the magnetic interaction of nuclei with orbital electrons, from which all the types of  $J$  coupling terms may be obtained, has been given elsewhere.<sup>29</sup> Ramsey and Purcell use this Hamiltonian and outline the origin and approximate magnitudes of the various coupling mechanisms. A paper by Ramsey<sup>30</sup> discusses and completes the formal analysis of these effects by a generalized treatment of the Hamiltonian which he used to explain the origin of the chemical shift.

<sup>29</sup> A. Abragam and M. H. L. Pryce, Proc. Roy. Soc. (London) A205, 135 (1951).

<sup>30</sup> N. F. Ramsey, Phys. Rev. 87, 1077 (1952). The authors are grateful to Professor Ramsey for an advance copy of this paper.

The  $\mathbf{I}_1 \cdot \mathbf{I}_2$  operator can be deduced by assuming that the wave packets representing two neighboring protons in a molecule overlap to a sufficient extent. However, this mechanism must be excluded because of mass considerations, especially since the  $J$  coupling is observed to involve nuclei much heavier than protons. We have considered a rotationally invariant form of magnetic interaction  $\mathbf{u}_1 \cdot \mathbf{u}_2$ , which can be obtained from the Hamiltonian which Ramsey used to explain the chemical shift.<sup>6</sup> For  $l$  nuclei interacting with  $k$  electrons this term is expressed as

$$\mathcal{E} = \frac{e^2}{2mc^2} \int \psi^*(\rho) \sum_k [\sum_l \gamma_l \mathbf{I}_l \times \mathbf{r}_{kl} / r_{kl}^3] \psi(\rho) d\rho, \quad (23)$$

where  $r_{kl}$  is the electron-nuclear distance and  $\psi(\rho)$  is the total electron wave function. In the case of two coupled protons the interaction energy may be estimated from a mechanism analogous to that which leads

to the Lamb diamagnetic correction.<sup>5</sup> Consider the dipole field  $H \sim \mu_1/r_k^3$  ( $\sim 10$  gauss) for a proton nucleus, which causes a Larmor precession of the  $k$ th electron. The resulting current produces a field  $H'$  at the position of a neighboring nucleus. A crude estimate of  $H'$  may be obtained by multiplying  $H$  by the Lamb diamagnetic correction factor ( $\sim 10^{-5}$ ) for the hydrogen atom, and a splitting of  $\sim 0.5$  cps is obtained. This splitting compares to the approximate value Drell has calculated<sup>31</sup> for this interaction in the HD molecule, using Heitler-London electron wave functions in Eq. (23). The small size of this splitting is of the order of magnitude of the splitting due to electron orbital contributions<sup>17</sup> and to cross terms due to direct dipole coupling between the electron and the nucleus.<sup>20</sup>

## VI. CONCLUDING REMARKS

Throughout this work we have studied shapes of echo envelopes under the rf pulse condition that  $\omega_1 t_w = \pi/2$ . Slight deviations from this condition will cause a marked deviation of the observed envelopes from the theoretical plots; the shape of the envelope depends critically on trigonometric terms which have quadratic and cubic dependence on the magnitude of  $H_1$ . The inhomogeneity of  $H_1$  over the sample is minimized by placing the sample in the center of a transmitter coil of larger diameter (three or four times as large as the receiver coil) where  $H_1$  is homogeneous. This is done most conveniently by fashioning the transmitter coil according to the Helmholtz condition, and crossing the transmitter and receiver at right angles according to the nuclear induction technique.<sup>2</sup>

Most of the compounds measured have involved relaxation times  $T_1$  and  $T_2$  of the order of several seconds, and in principle the parameters  $J$  and  $\delta$  of the order of  $1/T_2$  are resolvable. However, an inhomogeneous field  $H_0$  over the sample aggravates the damping effect due to thermal diffusion,<sup>14</sup> which becomes greater than the damping due to  $T_2$ , and it is important to shim the magnetic field sufficiently in order to obtain a reasonable field homogeneity.

The authors are grateful to Professor F. Bloch for many discussions and valuable suggestions during the course of this research. They wish to acknowledge the highly informative discussions and helpful interchange of information with Professors H. S. Gutowsky and C. P. Slichter of the University of Illinois. They thank Dr. S. D. Drell for discussions concerning some of the calculations, and Dr. M. E. Packard and Mr. J. T. Arnold for slow passage measurements of some of the compounds they studied. One of the authors (E.L.H.) wishes to acknowledge and thank the National Research Council for postdoctoral fellowship support during the early part of this research.

<sup>31</sup> S. D. Drell, private communication.

## APPENDIX

The echo at  $t=2\tau$  is given for the following cases, where groups  $A$  and  $B$  are at resonance:

(A)  $S_A = S_B = \frac{1}{2}$ ,  $I_A = I_B = \frac{1}{2}$ ,  $\gamma_A = \gamma_B$ ,  $\delta \sim J$  (Type  $\text{CHCl}_2\text{CHO}$ ):

$$|V| = \frac{M_0 \delta^2 \sin \varphi}{\delta^2 + J^2} \left| \left( \sin^2 \frac{\varphi}{2} \right) \left( \sin^2 \left[ \frac{\tau}{2} (J^2 + \delta^2)^{\frac{1}{2}} \right] \right) \cos J\tau \right. \\ \left. + \left( \frac{\sin^2 \varphi}{4} \right) \left\{ \frac{2J^2 + \delta^2}{\delta^2} + \cos[\tau(J^2 + \delta^2)^{\frac{1}{2}}] \right\} \right. \\ \left. - (\cos \varphi) \left( \sin^2 \frac{\varphi}{2} \right) \left( \frac{\cos J\tau}{2} \right) \left\{ 1 + \frac{2J^2 + \delta^2}{\delta^2} \right. \right. \\ \left. \left. \times \cos[\tau(J^2 + \delta^2)^{\frac{1}{2}}] \right\} + \frac{J(J^2 + \delta^2)^{\frac{1}{2}}}{\delta^2} \right. \\ \left. \times (\sin J\tau) \sin[\tau(J^2 + \delta^2)^{\frac{1}{2}}] \right|,$$

where  $\varphi = \omega_1 t_w$ .

(B)  $S_A = \frac{1}{2}$ ,  $S_B = 1$ ,  $I_A = I_B = \frac{1}{2}$ ,  $\gamma_A = \gamma_B$ ,  $\delta \sim J$ ,  $\omega_1 t_w = \pi/2$  (Type  $\text{CH}_2\text{ClCHCl}_2$ ):

$$|V| = \frac{1}{3^{\frac{1}{2}}} M_0 \left| [\bar{z}x(\bar{w} - 2w) - 2y(\bar{w}^2 - 2x^2)] \right. \\ \left. \times \exp[i\tau(\delta/2 + 3J/4)] + \text{c.c.} \right. \\ \left. + [\bar{z}x(y - 2\bar{y}) - 2\bar{w}(y^2 - 2\bar{z}^2)] \right. \\ \left. \times \exp[i\tau(\delta/2 - 3J/4)] + \text{c.c.} \right. \\ \left. + [wy - 2\bar{x}\bar{z}] \exp[-i3J\tau/2] + \text{c.c.} \right. \\ \left. + (4/3)x^2(y^2 + \bar{y}^2) + (10/3)x\bar{z}(w - \bar{w})(y - \bar{y}) \right. \\ \left. - 3(|w|^2 + |y|^2) - (8/3)|w|^2|y|^2 \right. \\ \left. + (15/3)x^2z^2 + (4/3)z^2(w^2 + \bar{w}^2) - (4/3) \right|,$$

where c.c. indicates the complex conjugate of the preceding expression, the bar over a symbol denotes the complex conjugate, and

$$w = \cos\left[\frac{1}{2}\tau(\delta^2 + \delta J + 9J^2/4)^{\frac{1}{2}}\right] + \frac{i(\delta/3 + 3J/2)}{(\delta^2 + \delta J + 9J^2/4)^{\frac{1}{2}}} \\ \times \sin\left[\frac{1}{2}\tau(\delta^2 + \delta J + 9J^2/4)^{\frac{1}{2}}\right], \\ x = \frac{-2i\delta\sqrt{2}}{3(\delta^2 + \delta J + 9J^2/4)^{\frac{1}{2}}} \sin\left[\frac{1}{2}\tau(\delta^2 + \delta J + 9J^2/4)^{\frac{1}{2}}\right], \\ y = \cos\left[\frac{1}{2}\tau(\delta^2 - \delta J + 9J^2/4)^{\frac{1}{2}}\right] - \frac{i(\delta/3 - 3J/2)}{(\delta^2 - \delta J + 9J^2/4)^{\frac{1}{2}}} \\ \times \sin\left[\frac{1}{2}\tau(\delta^2 - \delta J + 9J^2/4)^{\frac{1}{2}}\right], \\ z = \frac{2i\delta\sqrt{2}}{3(\delta^2 - \delta J + 9J^2/4)^{\frac{1}{2}}} \sin\left[\frac{1}{2}\tau(\delta^2 - \delta J + 9J^2/4)^{\frac{1}{2}}\right].$$

For  $J \ll \delta$  in this case,  $V$  reduces to

$$|V| = (M_0/48) \left| 11 + 12 \cos J\tau + \cos 2J\tau \right. \\ \left. + (8 \cos \delta\tau)(\cos J\tau/2 - \cos 3J\tau/2) \right|.$$

(C) The cases given below apply for  $I_A = I_B = \frac{1}{2}$ ,  $\gamma_A = \gamma_B$ ,  $J \ll \delta$ ,  $\omega_1 t_w = \pi/2$ :

(1)  $S_A = 1$ ,  $S_B = 1$ , (Type  $\text{CH}_2\text{ClCH}_2\text{Br}$ ):

$$|V| = \frac{1}{16} M_0 |3 + 4 \cos J\tau + \cos 2J\tau + 4 (\cos \delta\tau) \sin^2 J\tau|.$$

(2)  $S_A = \frac{3}{2}$ ,  $S_B = \frac{1}{2}$ , (Type  $\text{CH}_3\text{OH}$ ):

$$|V| = (M_0/224) |50 + \cos 3J\tau + 6 \cos 2J\tau + 55 \cos J\tau + (8 \cos \delta\tau)(2 + \cos J\tau - 3 \cos 2J\tau)|.$$

(3)  $S_A = \frac{3}{2}$ ,  $S_B = 1$ , (Type  $\text{CH}_3\text{CH}_2\text{Br}$ ):

$$|V| = (M_0/272) |45 + 66 \cos J\tau + 23 \cos 2J\tau + 2 \cos 3J\tau + (8 \cos \delta\tau) \times (5 \cos J\tau/2 - 2 \cos 3J\tau/2 - 3 \cos 5J\tau/2)|.$$

(4)  $S_A = 1$ ,  $S_B = 1$ , *except that*  $I_A = I_B = 1$ , (Type  $\text{CDCl}_2\text{CDO}$ ):

$$|V| = (M_0/12) |1 + 4 \cos J\tau + \cos 2J\tau + (4 \cos \delta\tau) \sin^2 J\tau|.$$

The cases below apply for three spin-groups  $A$ ,  $B$ , and  $C$ , where  $A$  and  $B$  are at resonance and  $C$  is off resonance ( $I_A = I_B = I_C = \frac{1}{2}$ ,  $\gamma_A = \gamma_B \neq \gamma_C$ ):

(5)  $S_A = S_B = S_C = \frac{1}{2}$ , (Type  $\text{CFHCICHCl}_2$ ):

$$|V| = \frac{1}{2} M_0 |\cos^2 J\tau/2 + (\sin^2 J\tau/2) \times (\cos[(K-L)\tau/2]) \cos \delta\tau|,$$

(6)  $S_A = S_B = \frac{1}{2}$ ,  $S_C = 1$ , (Type  $\text{CF}_2\text{HCHCl}_2$ ):

$$|V| = \frac{1}{2} M_0 |\cos^2 J\tau/2 + (\sin^2 J\tau/2) \times (\cos^2[(K-L)\tau/2]) \cos \delta\tau|,$$

where  $K$  and  $L$  denote the coupling of groups  $A$  and  $B$  with  $C$ .

(D) The solution of Eq. (20) is

$$F_n = \frac{iM_0\lambda'}{4(\lambda+\lambda')} e^{i(\omega_n+\omega_n')t-\lambda-\lambda't/2} \times \left[ 1 + \frac{\lambda+\lambda'+i\Delta\omega_n}{\alpha} \sinh\left(\frac{\alpha t}{2}\right) - e^{-\alpha t/2} \right],$$

where  $\Delta\omega_n = \omega_n - \omega_n'$  and

$$\alpha = [(\lambda+\lambda')^2 - \Delta\omega_n^2 - 2i(\lambda-\lambda')\Delta\omega_n]^{\frac{1}{2}}.$$

A similar solution exists for  $F_n'$ .  $F_n$  can be expanded and expressed in the form

$$F_n = \frac{iM_0\lambda'}{4(\lambda+\lambda')} \left\{ e^{(i\omega_n-\lambda)t+\lambda} \int_0^t e^{(i\omega_n-\lambda)t_1+(i\omega_n'-\lambda')(t-t_1)} dt_1 + \lambda\lambda' \int_0^t \int_0^{t-t_1} e^{(i\omega_n-\lambda)(t-t_2)+(i\omega_n'-\lambda')t_2} dt_2 dt_1 \right. \\ + \lambda^2 \lambda' \int_0^t \int_0^{t-t_1} \int_0^{t-t_1-t_2} e^{(i\omega_n-\lambda)(t_1+t_3)+(i\omega_n'-\lambda')(t-t_1-t_3)} dt_3 dt_2 dt_1 + \dots \\ + \lambda^k \lambda'^k e^{(i\omega_n-\lambda)t} \int_0^t \int_0^{t-t_1} \dots \int_0^{t-t_1-t_2-\dots-t_{2k-1}} e^{(i\Delta\omega_n-\lambda+\lambda')(t_2+t_4+t_6+\dots+t_{2k})} dt_{2k} dt_{2k-1} \dots dt_1 \\ \left. + \lambda^{k+1} \lambda'^k e^{(i\omega_n'-\lambda')t} \int_0^t \int_0^{t-t_1} \dots \int_0^{t-t_1-t_2-\dots-t_{2k}} e^{(i\Delta\omega_n-\lambda+\lambda')(t_1+t_3+t_5+\dots+t_{2k+1})} dt_{2k+1} dt_{2k} \dots dt_1 \right\}.$$

Each term of the expansion represents a mode of switching between two frequencies of precession  $\omega$  and  $\omega'$ . The first term of the expansion is determined by the probability  $e^{-\lambda t}$  that the ensemble precesses at a frequency  $\omega_n$  for a time  $t$ . The second term accounts for the probability  $(e^{-\lambda t_1} \lambda dt_1) e^{-\lambda'(t-t_1)}$  that the ensemble precesses at frequency  $\omega_n$  for a time between  $t_1$  and  $t_1+dt_1$ , then switches to the frequency  $\omega_n'$  and remains

for a time  $t-t_1$ . The third term includes the probability that the ensemble returns to frequency  $\omega_n$  and remains. Successive terms account for increasingly frequent jumps between frequencies  $\omega_n$  and  $\omega_n'$ . Each mode of interrupted precession is therefore weighted and the observed nuclear magnetization is a superposition of all modes. A similar argument applies to the expansion of  $F_n'$ .



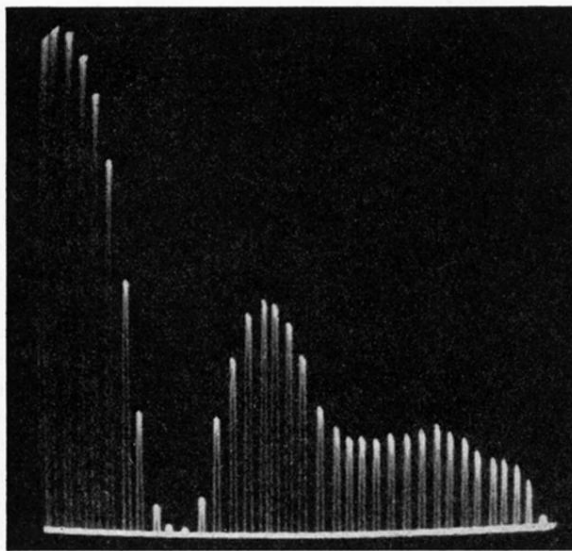


FIG. 1. Multiple photographic exposures of proton echo oscilloscope signals obtained in 2-bromo-5-chlorothiophene. The first rf pulse initiates the sweep. An exposure is made of the echo for each position of the second pulse (the pulses are not visible). As  $\tau$  is increased, the maximum of the spin echo at the time  $2\tau$  traces out the modulation of the echo envelope. The time duration of the total sweep is 0.66 sec, and the Larmor frequency is 31 Mc.

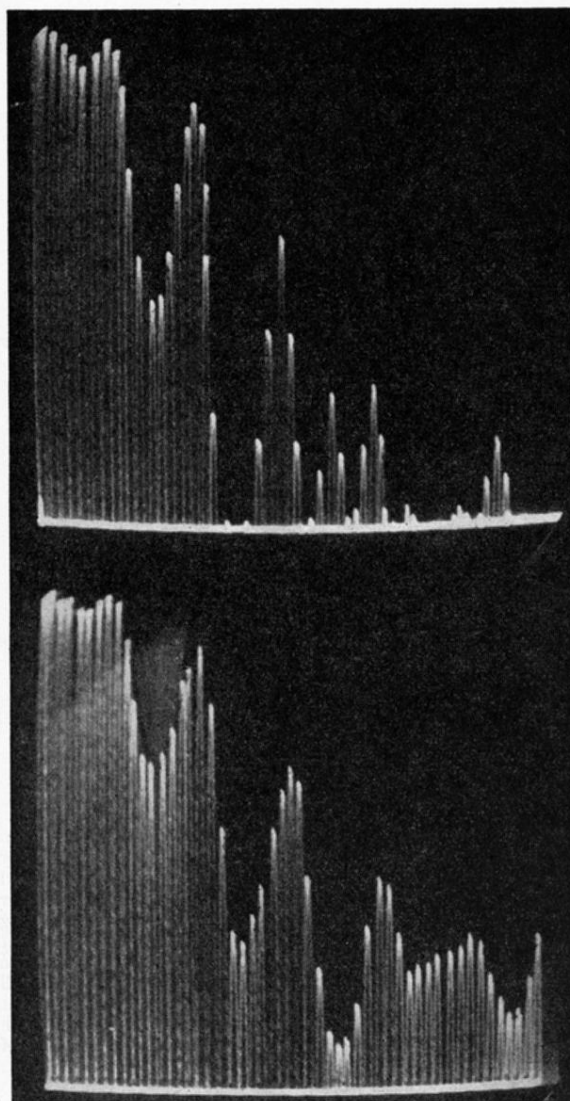


FIG. 5. The upper photograph shows the echo envelope due to protons in pure  $\text{CHCl}_2\text{CH}_2\text{Cl}$  at a Larmor frequency of 31 Mc. Both photographs are obtained by the method indicated in Fig. 1. The time duration of the total sweep is 0.22 sec. The lower photograph shows, on the same time scale as the upper one, the echo envelope due to protons in a mixture of  $\text{CHCl}_2\text{CH}_2\text{Cl}$  and chloroform ( $\text{CHCl}_3$ ). The echo modulation frequency doubling effect, which is seen in the pure compound above, does not appear below because the echo component produced by the protons in  $\text{CHCl}_3$  (which alone does not exhibit envelope modulation) serves as reference upon which the sinusoidal echo modulation due to  $\text{CHCl}_2\text{CH}_2\text{Cl}$  may superimpose. Thus, the total echo vector never reverses direction (see caption of Fig. 4).